Assessment of automatic hedgerow detection using Pleiades Neo 30cm spatial resolution images and Foundation model

Lea Moyon, Marie Ballere, Noe Roure, Anne Jacquin, David Souveton, Vincent Varoquaux, Alexandre Mayerowitz, Laurent Gabet

AIRBUS Defence and Space, 5 rue des satellites, 31030 Toulouse, France – lea.moyon@airbus.com, marie.ballere@airbus.com, noe.roure@airbus.com, anne.jacquin@airbus.com, david.souveton@airbus.com, vincent.varoquaux@airbus.com, alexandre.mayerowitz@airbus.com, laurent.gabet@airbus.com

Keywords: Hedgerows, Pleiades Neo, Foundation Model, Segmentation, Artificial Intelligence.

Abstract

Hedgerows, a traditional agroforestry practice, are declining in Europe, threatening biodiversity and climate control. To support high-quality agricultural carbon credit certification, a method for automatic hedge detection using Pleiades Neo 30cm satellite imagery was developed. Two methodological approaches were tested in three French study areas with varied landscapes: (i) a classic image segmentation using NDVI, Green Cover Fraction, and LiDAR-derived Digital Height Model, and (ii) a foundation model retrained on 150 annotated tiles. The methods were compared using quantitative and qualitative indicators. The foundation model demonstrated superior hedge detection and robustness across different landscapes. A ground truth dataset based on stratified random sampling and equal allocation was created to allow the quantification of its accuracy using standard metrics. The accuracy assessment was performed over 22 European study sites. It achieved a global accuracy of 87%, with a precision of 84% and a recall of 86% for the hedge class. It effectively adapted to the morphological and ecological diversity of hedges, with few commission errors primarily due to confusion with linear vegetation, and omissions mainly in discontinuous or degraded hedges. The study confirms the relevance of Pleiades Neo for detecting narrow features such as hedges, as well as the effectiveness of foundation models with limited reference data, and their potential for large-scale hedge mapping. Future work aims to expand the model’s training and incorporate atmospherically corrected RGB-NIR spectral band images to improve hedgerow detection across the European Union, paving the way for operational tools in agricultural carbon credit valuation.

1. Introduction

1.1 Context

Across Europe, the significant decline of hedgerow practices since the 1950s has had profound implications on biodiversity and ecosystem services. By 2016, the total area covered by agricultural hedges across the 27 EU countries was estimated at 1.78 million hectares, constituting 0.42% of the territory's surface (den Herder, 2016). The rate of decline varies across countries: those with a strong hedgerow tradition, such as Ireland, the United Kingdom, and Denmark, have lost between 50 and 70% of their hedge networks, while Mediterranean countries like Spain, Italy, and Portugal have experienced more limited losses.

Several factors contribute to this decline, including soil artificialization, hedge uprooting for maintenance or agricultural machinery, and biomass overexploitation. Land consolidation policies, particularly in the 1970s, have been notably responsible for a substantial reduction in the hedgerow network. However, hedges play a crucial role as ecological niches, providing essential ecosystem services and serving as reservoirs of biodiversity. They offer habitats, refuges, and breeding grounds for numerous species, and are involved in water and climate regulation, as well as carbon storage (Drexler et al., 2021).

Given their importance, the conservation, restoration, and certification of hedges have become increasingly critical. The Common Agricultural Policy (CAP) has encouraged the protection of hedges since 1990 and now attempts to ban their removal. In the context of climate change, efforts to reduce greenhouse gas emissions are increasingly accompanied by compensation initiatives. Carbon storage, particularly in agricultural soils, is a major challenge, as these soils play a key role as carbon sinks (Lal, 2004). Compensating farmers for the services they provide is crucial for perpetuating agroecological practices (Bossio et al., 2020).

A carbon credit represents a ton of equivalent CO_2 avoided or sequestered, which companies can generate through their own actions or acquire on the market (Schneider and Theuer, 2019). There is ongoing debate about the fair valuation of agricultural carbon credits, recognizing both the climatic value of the services provided and the work done by farmers to modify their practices.

Hedges are significant levers for carbon storage in soils and are integrated into some mechanisms for valuing carbon credits. However, the current system relies heavily on voluntary declarations, which are often unreliable and imply a heavy workload for data collection, verification, and diagnosis. To promote the certification of high-quality agricultural carbon credits, accurately detecting hedges is required (Chenu et al., 2019; Girardin et al., 2021).

This contribution has been peer-reviewed.
https://doi.org/10.5194/isprs-archives-XLIX-B3-2026-633-2026 |

1.2 Related work

Hedges are thin linear elements of trees or shrubs, with, according to which definition is used, criteria on height, length or discontinuity. Studies using satellite imagery have demonstrated its relevance for detecting small woody elements, including hedges (Vannier and Hubert-Moy, 2010). Given the thin nature of these elements, very high resolution (VHR) imagery (spatial resolution less than 1m) is pertinent. Research has also shown the effectiveness of combining multispectral data with active sensor data, such as Light Detection and Ranging (LiDAR), to enhance the delineation and characterization of vegetation height and density (Broughton et al., 2021; Popescu et al., 2003; Rosier et al., 2021; Malinowski, 2016).

Hedges exhibit specific spectral characteristics that can be exploited through spectral indices and biophysical variables derived from passive multispectral sensors (Xie et al., 2008). The Normalized Difference Vegetation Index (NDVI) is the most commonly used index, evaluating photosynthetic activity and identifying densely vegetated areas (Rouse et al., 1974). However, NDVI's tendency to saturate in dense vegetation limits its effectiveness in distinguishing thick hedges (Huete et al., 2002; Gitelson, 2004). To refine detection, other indices such as the Canopy Shadow Factor (CSHN), Soil Adjusted Vegetation Index (SAVI), Difference Vegetation Index (DVI), Fractional Vegetation Cover (FVC), Normalized Difference Fraction Index (NDFI), Chlorophyll concentration (CHL), Leaf Area Index (LAI), and Green Leaf Cover Value (GLCV) have been used. These indices provide information on vegetation cover, photosynthetic activity, biomass volume, and structural development, aiding in the differentiation of hedges from other covers (Xie et al., 2008; Huete, 1988; Tucker, 1979; Carlson and Ripley, 1997; Baret et al., 2007; Delgado-Moreno and Gao, 2022; Gitelson et al., 2003; Delegido et al., 2013; Myneni et al., 2002; Garrigues et al., 2008).

Once extracted, these indices can be used in various hedge mapping approaches, whether based on image segmentation, machine learning (ML) or deep learning (DL) methods. Historically, the identification and mapping of hedges relied on manual photo-interpretation of aerial images, supplemented by field surveys (Pasher et al., 2016; Hölbling et al., 2017; Oldeland et al., 2021). However, these methods have limitations in terms of spatial extent, revisit frequency, cost and automation capacity. Traditional image segmentation techniques based on height data or spectral indices have been used for large-scale mappings but lack precision and efficiency compared to ML and DL models (Broughton et al., 2021; Pasher et al., 2016).

In a pixel-oriented approach, the spectral signatures and values for certain indices of hedges can be similar to those of other tree formations, such as forests, groves, or isolated trees. The linear geometry of hedges makes them suitable for object-oriented analysis, but this characteristic can also lead to confusion with other linear elements in the landscape, such as roads, paths, or walls (Vannier and Hubert-Moy, 2010; Pirbasti et al., 2024). Supervised learning methods oriented towards objects, such as support vector machine (SVM) classifiers and decision tree algorithms like Random Forest, have shown good detection performance in areas where the hedge structure is similar to the training data (Fauvel et al., 2014; Tansey et al., 2009; Aksoy et al., 2010; O'Connell et al., 2015). However, these approaches have limitations in terms of scalability and generalization where hedge density, species, or volume differ from the training data (Tansey et al., 2009; Valero et al., 2010; Pelletier et al., 2019).

Unsupervised deep learning models, such as pre-trained convolutional neural networks (CNNs) like DeepLab v3+ (Chen et al., 2018) and approaches based on Graph Neural Networks (GNNs), have improved performance and robustness (Zhu et al., 2017; Zhou et al., 2020). However, some heterogeneous classes remain difficult to isolate. For instance, Kattenborn et al. (2019) note that CNNs on multispectral images can confuse hedges with other woody structures such as groves or forest edges due to the lack of global spatial context (Wang et al., 2022).

Foundation models (FMs) represent a significant recent evolution in the field of image segmentation (Xiao et al., 2025). These models are designed and pre-trained on large volumes of heterogeneous unlabelled data, including satellite images. One of the main advantages of these models is their generalization capacity enabled by self-supervised learning. It allows producing robust predictions while reducing dependence on annotated datasets, which are often costly to assemble. Thus, FMs can offer better transferability and adaptability to different contexts, which is particularly relevant for detecting heterogeneous vegetation structures such as hedges.

In summary, the mapping of hedgerows has evolved from historically manual methods to automated approaches based on ML and DL methods. Foundation models have emerged as a promising solution for their generalization capacity and robustness, presenting strong potential for hedge detection.

1.3 Problem statement

The potential of the foundation model for detecting agroecological structures such as hedges is quite new and needs reference.

In our study, we started by conducting a comparative analysis on hedge detection between two methods developed across various hedge contexts in France: a traditional segmentation method and a foundation model. Then, we tested the foundation model on diverse European study sites to encompass a wide range of landscape contexts, seasons, and image acquisition conditions. These methods were based on very high-resolution Pléiades Neo satellite imagery, as the small details of hedges require such resolution.

In this study, hedges are defined as linear vegetation formations with a maximum width of 20 meters, without length or height restrictions, and a maximum discontinuity of 5 meters. This definition was selected after reviewing several definitions used in European certification and legislative contexts, as it is comprehensive and aligns with the preference for over-detection rather than omission in most regulatory frameworks.

2. Study area

For the development and the comparison of the traditional segmentation methodology and the foundation model, three French study sites were selected to assess hedge detection potential in various landscapes. The first is located in the Maine-et-Loire department, a flat grassland region characterized by a historically dense and continuous hedge network. The second and third study areas are in the Doubs and Puy-de-Dôme departments, hilly regions with more pronounced topography. In Doubs, hedges are generally sparse and fragmented, while the Puy-de-Dôme area offers an intermediate hedge structure and typology between the other study sites. All three regions are livestock breeding areas, featuring landscapes composed of a mosaic of forests, grasslands, and hedges.

https://doi.org/10.5194/isprs-archives-XLIX-B3-2026-633-2026 |

To test the generalization of the foundation model, we carefully selected 22 study sites across Europe, spanning 18 different countries (Figure 1). This selection was made to ensure a wide diversity of agricultural practices and landscapes. The chosen sites encompass a variety of climates, including continental regions (6 sites, totalling 2140 km²), oceanic areas (8 sites, covering 1600 km²), Mediterranean or warm temperate zones (5 sites, representing 535 km²), as well as mountainous regions (3 sites, extending over 477 km²). This approach allows us to evaluate the robustness and adaptability of the model under varied environmental and agricultural conditions, providing a comprehensive understanding of its effectiveness across Europe.

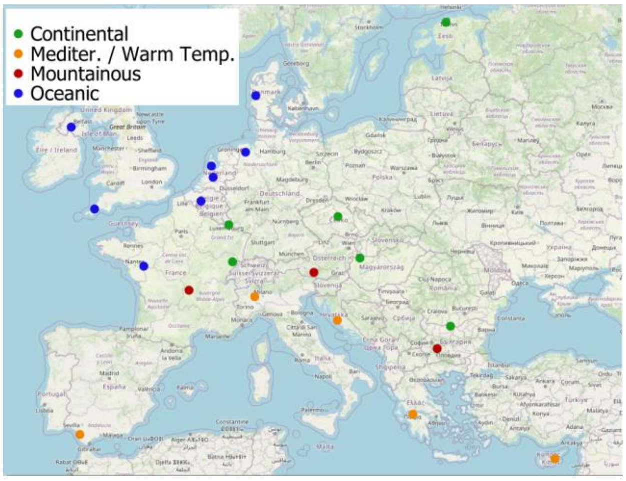

Figure 1. Location of study sites across Europe. © OpenStreetMap contributors, ODbL licence.

3. Data

With their six spectral bands and 30cm spatial resolution, Pleiades Neo images are particularly well suited for object detection in which radiometry is as important as texture and shape, which includes hedges. For each test area, we selected one Pleiades Neo image from ©OneAtlas Basemap, Airbus DS (based on Airbus Defence & Space satellite constellation imagery), ensuring seasonal coverage with six images from winter, six from spring, six from summer, and four from autumn. They encompass a range of incidence angles: six images with angles between 0 and 10 degrees, eight between 10 and 20 degrees, and eight with angles exceeding 20 degrees. The selected images are orthorectified but not corrected from atmospheric effects. Specifically, the images chosen over France were selected to closely match the acquisition dates of the Lidar HD data (IGN) used to derive a Digital Height Model. This temporal alignment allows us to test traditional segmentation methods effectively.

To include vegetation height in the segmentation method, we incorporated the high-resolution LiDAR HD data provided by the French National Institute of Geographic and Forest Information (IGN). This dataset offers complete LiDAR coverage of metropolitan France at a 50 cm resolution. The IGN LiDAR data, available under an open license on the IGN website, can be freely downloaded (https://geoservices.ign.fr/lidarhd).

4. Method

Two methodological approaches to detect hedges were developed over the three French study sites, each with different configurations.

4.1 Segmentation

The first methodology tested for hedge detection involved image segmentation using biophysical variables and height data.

Following a literature review, five biophysical indices were selected for their relevance in detecting hedgerows: NDVI, CHL, CSHN, NDFI, and GLCV. These variables were produced using Overland, a software developed by Airbus DS (Poilvé, 2010). This tool characterizes soils and vegetation cover through the inversion of reflectance models (SAIL/PROSPECT for vegetation response modelling and LOWTRAN/MODTRAN for atmospheric modelling). LiDAR data was downloaded from the IGN portal to construct the Digital Height Model (DHM), and a slight offset between the DHM and PNEO image was corrected through image registration.

Individual variables were first analysed to assess their ability to differentiate hedges from other landscape elements. Variables were then combined, and thresholds were adjusted to optimize hedge detection using photo-interpretation. The CHL showed similar discrimination to GLCV, likely due to their shared characteristics: both calculate metrics related to chlorophyll concentration and photosynthetic activity and are influenced by vegetation density. However, GLCV proved slightly more precise on the test images, leading to its selection. NDFI was discarded as it failed to discriminate between hedges, even partially, and other features. The most effective combination was DHM (2.5-10m), NDVI (0.3-0.8), and GLCV (0.4-1), with NDVI identifying vegetation and GLCV targeting medium to high-density structures.

Post-processing steps included forest masking with an external layer and morphological operations to fill gaps and remove isolated pixels. Linearity of objects was ensured by applying a morphological filter to retain only linear objects of at least 5 pixels in length and 1 pixel in width, and using a connected finesse index (Jiao and Liu, 2012) to remove isolated trees.

In summary, this first segmentation method combines DHM, NDVI, and GLCV for hedge detection, followed by morphological operations and geometric index application to refine results. This approach optimizes hedge detection while minimizing noise and artifacts.

4.2 Foundation model

The second method is based on RGB images and a foundation model developed by Airbus DS. To adapt the foundation model for the purpose of hedge detection, we fine-tuned it using a limited set of labels. The Airbus foundation model is based on a ViT architecture with approximately 900 million parameters. It has been initially pre-trained for multi-task segmentation on a dataset of more than 10,000 image tiles of 1024 × 1024 pixels derived from high-resolution remote sensing imagery containing more than 1,000,000 masks.

The foundation model is then fine-tuned to be adapted to the hedge detection use case. To achieve this, we followed the workflow described below.

First, 15 Pleiades Neo images were selected to cover a wide diversity of European landscapes including hedges and various acquisition conditions. This diversity of images improves the robustness of the model across heterogeneous environments.

Second, the annotation work is performed using a custom annotation tool, providing a simple graphical user interface in which users can directly interact with image segmentation masks. The tool is integrated within an active learning workflow. After a short initial round of manual annotations, the foundation model is fine-tuned and applied to the dataset to generate predictions. Users then correct the predicted masks, and the system records the locations where corrections are made. During subsequent training iterations, higher loss weights are applied to pixels corresponding to human corrections, increasing the influence of corrected regions and accelerating model improvement. This human-in-the-loop procedure was repeated for four iterations leading to the final training dataset of 150 annotated tiles with diverse landscapes and satellite acquisition configurations.

Model training uses the AdamW optimizer (Loshchilov and Hutter, 2017) with a learning rate of 1×10-5 and a weight decay of 1×10-4. To improve generalization and robustness to varying image conditions, several data augmentation techniques were applied during training, including for example color jitter, contrast modification, cloud simulation, random cropping, rotation, Gaussian blur, etc. (Laskin et al., 2020)

This iterative active learning process enables rapid improvement of the segmentation performance while limiting the amount of manual labeling required. It also allows to quickly validate model performance at large scale and efficiently generate improved model versions throughout the annotation cycle.

Finally, the inference of the foundation model on an image results in a probability of hedge presence for each pixel. To obtain the hedge detection, a threshold is applied to this probability. Based on the analysis conducted across the three French study sites, the threshold was set at 0.7. Pixels with probabilities exceeding this threshold are classified as hedges, while those below are classified as non-hedges.

4.3 Metrics for methods comparison

The performance of each method was compared over the three French study sites using quantitative metrics (Intersection Over Union and pixel count detected by a single method) and visual inspection.

4.4 Metrics for accuracy assessment

The objective is to validate the generalization of hedge models across various landscape contexts, climatic zones, seasons, and image parameters. To achieve this, reference datasets were created using stratified random sampling to ensure sufficient statistical representation of each map class (Olofsson et al., 2014).

A total of more than 5300 samples of “hedges” and “non-hedges” were produced. First, we used points sampled during the experiment over the three French test sites. Then, for all other test sites, 900 points were sampled per climatic zone (continental, oceanic, Mediterranean/warm temperate, and mountainous). This number of samples was determined using Cochran's formula (Cochran, 1977). To calculate the number of points sampled per test site within each climatic zone, its surface area and hedgerow proportion was considered in relation to other sites within its climate category, with a minimum of 30 “hedges” and 30 “non-hedges” points per site. Stratification was based on the mapped classes. Sample allocation was done equally following recommendations of Olofsson et al (2014) to validate the accuracy of each class. Samples were then randomly selected within the two strata and labelled through human photo-interpretation based on optical imagery, using Google Earth Pro version 7.3.3.7786 (2020) and ©OneAtlas Basemap, AIRBUS DS images.

This reference dataset was used to quantify the accuracy of hedge detection with standard accuracy metrics (overall accuracy, Cohen Kappa index and accuracy, recall, F1-score specific for hedge class). Confusion matrices and metrics were computed globally, per climatic zone, per season and per incidence angle.

5. Results

5.1 Methods comparison

The two methodological approaches provide very different results with an Intersection over Union between results from first and second methods ranging from 11% to 21% according to the study sites (Figure 2).

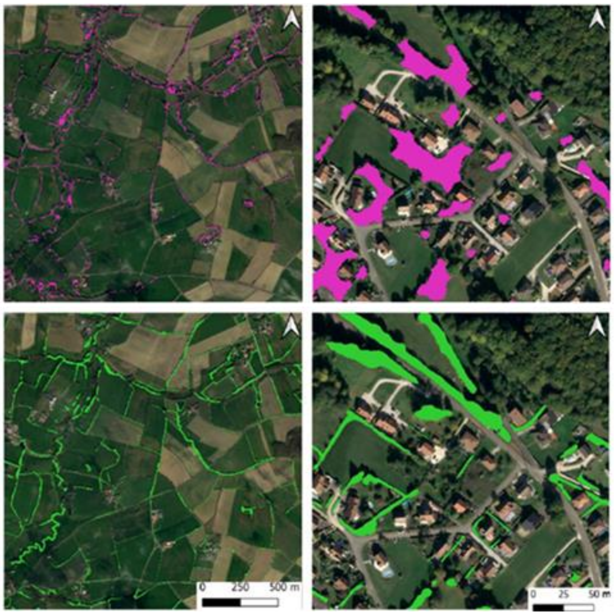

Figure 2. Example of hedge map obtained with, above, the segmentation approach and below, the foundation model specifically pre-trained for hedges.

The number of pixels detected only by the segmentation method ranges between 16 and 45%, while it ranges between 34 and 72% for the foundation model.

Visual inspection reveals that the first method significantly overestimates and misses hedges. Confusion can arise with other vegetal structures, isolated trees, or vegetation shadows: the method tends to integrate them as part of the hedge, leading to misclassification. Additionally, the methodology detects vegetation with a shape very close to the hedge definition and tends to insert continuity between neighbouring hedges or between hedges and isolated trees. This artifact results in the detection of incorrect shapes, often too wide. It is primarily found in urban/semi-urban areas, particularly in gardens.

The second method misses as well very few hedges with 0.5% omission error. It detects hedges with less fragmentation than with the first method. The result is close to what is observed in the landscape. Finally, the method does not over-estimate hedges. The foundation model shows a good adaptation capacity to the wide morphological and ecological varieties of the hedges. For all these reasons, the second method offers the best hedgerow detection. It is the most robust when faced with different landscape contexts.

5.2 Hedge detection with the foundation model

The quantitative analysis, based on a reference dataset of 5300 samples, demonstrates an overall accuracy of 87%, with an accuracy of 84% and a recall of 86% at the European scale (Figure 3). This indicates a good detection rate. Across all contexts, the overall accuracy exceeds 84%, regardless of climatic zone, season, or incidence angle (Figure 4). This demonstrates the model's good capacity to generalize across Europe, seasons, and acquisition parameters.

When considering different climatic zones, accuracy varies between 80% and 91%. Recall is above 85% for all climatic zones, indicating a high detection rate, except for the Mediterranean/warm temperate climate, which exhibits a lower recall of 73%. This may be attributed to the threshold applied to the probability map of hedge presence used to binarize the map. This threshold was defined over the French sites located in continental, oceanic, and mountainous regions. Adjusting the detection threshold specifically for the Mediterranean/warm temperate zone could potentially increase the detection rate, even with a slight increase in commission errors, which currently stand at 8%.

Seasonal analysis reveals that the overall accuracy for winter, autumn, and summer is comparable, ranging from 85% to 87%. Spring, however, shows superior performance with an overall accuracy of 91%, an accuracy of 92% and a recall of 88%.

The analysis of different angles of incidence does not indicate a clear preference for any specific category. While precision increases with the incidence angle (79% for 0-10°, 85% for 10-20°, and 91% for 20-30°), the detection rate (recall) does not follow a consistent pattern. It remains above 88% for most categories, except for the 10-20° category, where it drops to 78%.

A visual analysis facilitated the identification of detection errors, which can be categorized into three distinct groups.

The first group concerns hedge detection errors resulting from the fact that the model predominantly relies on the contextual information to detect a hedge. This led to both:
1) commission errors: confusions were found with elements that create texture, such as tall herbaceous vegetation, soil roughness, or soil moisture, and that present a linear shape. It was observed, for example, in Northern European landscapes where grassy embankments, ditches, and canals tend to cast shadows and, consequently, can resemble hedges;
2) omission errors: it was observed in two cases. First, deciduous tree alignments in winter are leafless which make them almost transparent despite the presence of the trunks and therefore, are difficult to recognize as a hedge. It should be noted that in the cases where they are mis-detected as hedges, this particular hedge-observation configuration can lead to issues in hedge delineation. Second, when textured elements wrongly assimilated to hedges are adjacent to true hedges, the resulting global element is not considered as a hedge as it does not fit anymore to the hedge definition.

These errors show that the context has a stronger impact on the detection of a hedge than the spectral information itself.

Figure 3. Example of hedges map obtained with the foundation model over different context: a) Denmark (oceanic climate, image of November, at 11.8° of incidence angle); b) Greece (Mediterranean climate, image of March, at 29.8° of incidence angle); c) United Kingdom (oceanic climate, image of July, at 1.5° of incidence angle).

The second group corresponds to hedge detection errors due to the conditions of observation affecting essentially the hedge delineation quality. First, the model's training was conducted in a way that shadows would not be considered as hedges. Nevertheless, a few confusions were observed with shadows of hedge vegetation integrated into the hedge element. This phenomenon is stronger in winter and at high latitudes, where shadows are larger. Second, increased incidence angles displaced the hedge location, affecting the accuracy of the hedge delineations.

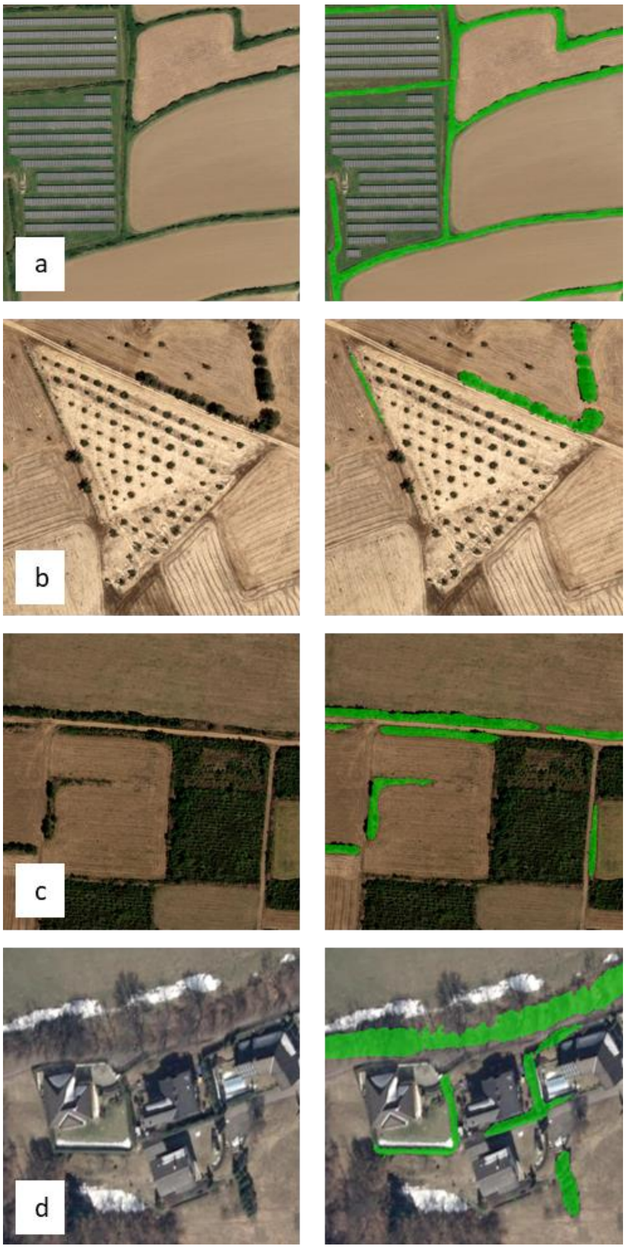

Figure 4. Example of hedges features obtained with the foundation model:a) United Kingdom (oceanic climate, image of July, at 1.5° of incidence angle); b) Cyprus (Mediterranean climate, image of June, at 13° of incidence angle); c) Bulgaria (continental climate, image of September, at 24.9° of incidence angle); d) Austria (mountainous climate, image of January, at 29.6° of incidence angle).

The last group gathers hedge detection errors related to the hedge characteristics. Indeed, some errors come from tree alignments for which the discontinuity is greater than 5 meters, or woody features larger than 20 meters (such as riparian forests). The verification of these criteria is challenging, considering the variability of the image acquisition parameters. Operator sensitivity in annotation and validation led to inconsistencies in classifying linear structures near plantations, forest patches, or isolated trees (which may or may not meet the discontinuity criterion). Notably, discontinuity-related errors were absent in typical hedgerow landscapes of Ireland and Great Britain. These latter are characterized by historical, managed hedges, as they have fewer natural hedges that may be at the borderline of the discontinuity criterion.

6. Discussion

6.1 Improvement of hedge detection

In several use cases, detecting hedges is sufficient without requiring a precise delineation of their contours. In this regard, a linear feature could be generated by skeletonizing the segmentation from the base model, thus reducing errors related to incidence angles and shadows (second group of errors). Then, a way to improve the model segmentation result itself would be to enrich the training label dataset by integrating examples representative of the observed errors, mainly for the first group. However, this approach would still be based on contextual information. We have found that the first group of errors could be avoided by exploiting the radiometry of the pixels in a more systematic manner, particularly for embankments, ditches, and low vegetation. In this context, it would be relevant to evaluate the interest to use atmospherically corrected RGB-NIR (Near Infrared) Pléiades Neo images. Using Top-Of-Canopy radiometry corrected images should improve the quality of the reflectance and give more weight to the intrinsic information of the pixel. Adding the NIR band should solve confusions with canals, ditches, and low vegetation. However, the base model, trained on millions of RGB images, will require a very large training image database including these spectral bands and atmospheric correction for their information to have weight. Despite these improvements, errors related to the definition of hedges (third group) seem particularly challenging to eliminate. A way for improvement would be to adapt the binarization threshold of the hedge presence probability map according to the landscape or climatic zone, in order to optimize results, especially in Mediterranean or warm temperate regions.

6.2 Hedge delineation

Hedge delineation can be needed for hedges characterization, for example for their biomass estimation. It is also essential when tracking the spatial evolution of hedges over time. We have observed that factors such as the angle of incidence, shadows, and the absence of leaves on hedges during winter can lead to delineation errors. For this purpose, it might be necessary to establish criteria on conditions for observation of the images used. Specifically, it is advisable to prioritize images taken outside periods when trees are leafless in regions with non-persistent foliage. Additionally, images with low incidence angles should be favoured to avoid hedge distortion.

7. Conclusion

The conclusions of this study confirm: i) the relevance of using Pléiades Neo for imaging thin-scale elements such as hedges, ii) the ability for foundation model to be trained with limited data and a few-shot learning, offering significant improvements over traditional methods, and iii) the potential of foundation model-based approaches for generalization and large-scale mapping of hedges, paving the way for their integration into operational tools for valuing hedges in agricultural carbon credits for example. In this perspective, future work aims to expand the model's training and incorporate atmospherically corrected images enriched with the NIR spectral band in addition to the RGB bands.

Ultimately, working to up-scale the European model at global scale seems to be relevant. Beyond the Western Europe context, in South America and in Asia, hedges or similar objects such as live fences and agroforestry hedgerows play important ecological and agronomic roles in farming systems.

Acknowledgements

This work is part of the CAFAMORE project that has received funding from the Horizon Europe Programme under Grant Agreement No. 101219027. It was co-founded by Airbus Defence and Space.

We would like to express our sincere gratitude to Elizabeth Langlois and Michael Tonon for their thorough review and valuable feedback on this manuscript.

References

Aksoy, S., Akcay, H.G., Wassenaar, T., 2010: Automatic Mapping of Linear Woody Vegetation Features in Agricultural Landscapes Using Very High Resolution Imagery, IEEE Transactions on Geoscience and Remote Sensing, 48(1), pp. 511–522. doi.org/10.1109/TGRS.2009.2027702.

Baret, F., Hagolle, O., Geiger, B., Bicheron, P., Miras, B., Huc, M., Berthelot, B., Niño, F., Weiss, M., Samain, O. and Roujean, J.L., 2007. LAI, fAPAR and fCover CYCLOPES global products derived from VEGETATION: Part 1: Principles of the algorithm. Remote sensing of environment, 110(3), pp.275-286. doi.org/10.1016/j.rse.2007.02.018.

Bossio, D.A., Cook-Patton, S.C., Ellis, P.W., Fargione, J., Sanderman, J., Smith, P., Wood, S., Zomer, R.J., Von Unger, M., Emmer, I.M. and Griscom, B.W., 2020. The role of soil carbon in natural climate solutions. Nature Sustainability, 3(5), pp.391-398. doi.org/10.1038/s41893-020-0491-z.

Broughton, R.K., Chetcuti, J., Burgess, M.D., Gerard, F.F. and Pywell, R.F., 2021. A regional-scale study of associations between farmland birds and linear woody networks of hedgerows and trees. Agriculture, Ecosystems & Environment, 310, p.107300. doi.org/10.1016/j.agee.2021.107300.

Carlson, T.N. and Ripley, D.A., 1997. On the relation between NDVI, fractional vegetation cover, and leaf area index. Remote sensing of Environment, 62(3), pp.241-252. doi.org/10.1016/S0034-4257(97)00104-1.

Chen, L.C., Zhu, Y., Papandreou, G., Schroff, F. and Adam, H., 2018. Encoder-decoder with atrous separable convolution for semantic image segmentation. In Proceedings of the European conference on computer vision (ECCV) (pp. 801-818). doi.org/10.48550/ARXIV.1802.02611.

Chenu, C., Angers, D.A., Barré, P., Derrien, D., Arrouays, D. and Balesdent, J., 2019. Increasing organic stocks in agricultural soils: Knowledge gaps and potential innovations. Soil and Tillage Research, 188, pp.41-52. doi.org/10.1016/j.still.2018.04.011.

Cochran, W.G., 1977. Sampling Techniques. 3rd Edition, John Wiley & Sons, New York.

Delegido, J., Verrelst, J., Meza, C.M., Rivera, J.P., Alonso, L. and Moreno, J., 2013. A red-edge spectral index for remote sensing estimation of green LAI over agroecosystems. European Journal of Agronomy, 46, pp.42-52. doi.org/10.1016/j.eja.2012.12.001.

Delgado-Moreno, D. and Gao, Y., 2021, November. Forest degradation estimation through trend analysis of annual time series NDVI, NDMI and NDFI (2010–2020) using landsat images. In International Conference on Geospatial Information Sciences (pp. 149-159). Cham: Springer International Publishing. doi.org/10.1007/978-3-030-98096-2_11.

Den Herder, M., Moreno, G., Mosquera-Losada, R.M., Palma, J.H., Sidiropoulou, A., Freijanes, J.J.S., Crous-Duran, J., Paulo, J.A., Tomé, M., Pantera, A. and Papanastasis, V.P., 2017. Current extent and stratification of agroforestry in the European Union. Agriculture, Ecosystems & Environment, 241, pp.121-132. doi.org/10.1016/j.agee.2017.03.005.

Drexler, S., Gensior, A., Don, A., 2021. Carbon sequestration in hedgerow biomass and soil in the temperate climate zone. Regional Environmental Change, 21(3), 74. doi.org/10.1007/s10113-021-01798-8

Fauvel, M., Planque, C., Sheeren, D. and Dalla Mura, M., 2014. Télédétection des éléments semi-naturels: utilisation des données Pléiades pour la détection des haies. Revue française de photogrammétrie et de télédétection, (208), pp.111-116. doi.org/10.52638/rfpt.2014.101.

Garrigues, S., Lacaze, R., Baret, F.J.T.M., Morisette, J.T., Weiss, M., Nickeson, J.E., Fernandes, R., Plummer, S., Shabanov, N.V., Myneni, R.B. and Knyazikhin, Y., 2008. Validation and intercomparison of global Leaf Area Index products derived from remote sensing data. Journal of Geophysical Research: Biogeosciences, 113(G2). doi.org/10.1029/2007JG000635.

Girardin, C.A., Jenkins, S., Seddon, N., Allen, M., Lewis, S.L., Wheeler, C.E., Griscom, B.W. and Malhi, Y., 2021. Nature-based solutions can help cool the planet—if we act now. Nature, 593(7858), pp.191-194. doi.org/10.1038/d41586-021-01241-2.

Gitelson, A.A., 2004. Wide dynamic range vegetation index for remote quantification of biophysical characteristics of vegetation. Journal of plant physiology, 161(2), pp.165-173. doi.org/10.1078/0176-1617-01176.

Gitelson, A.A., Gritz, Y. and Merzlyak, M.N., 2003. Relationships between leaf chlorophyll content and spectral reflectance and algorithms for non-destructive chlorophyll assessment in higher plant leaves. Journal of plant physiology, 160(3), pp.271-282. doi.org/10.1078/0176-1617-00887.

Hölbling, D., Eisank, C., Albrecht, F., Vecchiotti, F., Friedl, B., Weinke, E. and Kociu, A., 2017. Comparing manual and semi-automated landslide mapping based on optical satellite images from different sensors. Geosciences, 7(2), p.37. doi.org/10.3390/geosciences7020037.

Huete, A., Didan, K., Miura, T., Rodriguez, E.P., Gao, X. and Ferreira, L.G., 2002. Overview of the radiometric and biophysical performance of the MODIS vegetation indices. Remote sensing of environment, 83(1-2), pp.195-213. doi.org/10.1016/S0034-4257(02)00096-2.

Huete, A.R., 1988. A soil-adjusted vegetation index (SAVI). Remote sensing of environment, 25(3), pp.295-309. doi.org/10.1016/0034-4257(88)90106-X.

Jiao, L. and Liu, Y., 2012. Analyzing the shape characteristics of land use classes in remote sensing imagery. ISPRS Annals of the Photogrammetry, Remote Sensing and Spatial Information Sciences, 1, pp.135-140. doi.org/10.5194/isprsannals-I-7-135-2012.

Kattenborn, T., Eichel, J. and Fassnacht, F.E., 2019. Convolutional Neural Networks enable efficient, accurate and fine-grained segmentation of plant species and communities from high-resolution UAV imagery. Scientific reports, 9(1), p.17656. doi.org/10.1038/s41598-019-53797-9.

Lal, R., 2004. Soil carbon sequestration impacts on global climate change and food security. science, 304(5677), pp.1623-1627. doi.org/10.1126/science.1097396.

Laskin, M., Lee, K., Stooke, A., Pinto, L., Abbeel, P. and Srinivas, A., 2020. Reinforcement learning with augmented data. Advances in neural information processing systems, 33, pp.19884-19895.

Loshchilov, I. and Hutter, F., 2017. Decoupled weight decay regularization. arXiv preprint arXiv:1711.05101.

Malinowski, R., 2016. Research and development in the use of LIDAR elevation data for mapping of landscape elements including hedgerows, ditches and dikes. Report.

Myneni, R.B., Hoffman, S., Knyazikhin, Y., Privette, J.L., Glassy, J., Tian, Y., Wang, Y., Song, X., Zhang, Y., Smith, G.R. and Lotsch, A., 2002. Global products of vegetation leaf area and fraction absorbed PAR from year one of MODIS data. Remote sensing of environment, 83(1-2), pp.214-231. doi.org/10.1016/S0034-4257(02)00074-3.

O'Connell, J., Bradter, U. and Benton, T.G., 2015. Wide-area mapping of small-scale features in agricultural landscapes using airborne remote sensing. ISPRS Journal of Photogrammetry and Remote Sensing, 109, pp.165-177. doi.org/10.1016/j.isprsjprs.2015.09.007.

Oldeland, J., Revermann, R., Luther-Mosebach, J., Buttschardt, T. and Lehmann, J.R., 2021. New tools for old problems comparing drone-and field-based assessments of a problematic plant species. Environmental Monitoring and Assessment, 193(2), p.90. doi.org/10.1007/s10661-021-08852-2.

Olofsson, P., Foody, G.M., Herold, M., Stehman, S.V., Woodcock, C.E. and Wulder, M.A., 2014. Good practices for estimating area and assessing accuracy of land change. Remote sensing of Environment, 148, pp.42-57. doi.org/10.1016/j.rse.2014.02.015.

Pasher, J., McGovern, M. and Putinski, V., 2016. Measuring and monitoring linear woody features in agricultural landscapes through earth observation data as an indicator of habitat availability. International journal of applied earth observation and geoinformation, 44, pp.113-123. doi.org/10.1016/j.jag.2015.07.008.

Pelletier, C., Webb, G.I. and Petitjean, F., 2019. Temporal convolutional neural network for the classification of satellite image time series. Remote Sensing, 11(5), p.523. doi.org/10.3390/rs11050523.

Pirbasti, M.A., McArdle, G. and Akbari, V., 2024. Hedgerows monitoring in remote sensing: a comprehensive review. Ieee Access, 12, pp.156184-156207. doi.org/10.1109/ACCESS.2024.3485512.

Poilvé, H., 2010. geoland2 - BioPar Methods Compendium of MERIS FR Biophysical Products; p.45. doi:10.13140/2.1.4205.1843.

Popescu, S.C., Wynne, R.H. and Nelson, R.F., 2003. Measuring individual tree crown diameter with lidar and assessing its influence on estimating forest volume and biomass. Canadian journal of remote sensing, 29(5), pp.564-577. doi.org/10.5589/m03-027.

Rosier, I., Diels, J., Somers, B. and Van Orshoven, J., 2021. A workflow to extract the geometry and type of vegetated landscape elements from airborne LiDAR point clouds. Remote Sensing, 13(20), p.4031. doi.org/10.3390/rs13204031.

Rouse, J.W. et al., 1974. Monitoring vegetation systems in the Great Plains with ERTS, in. ntrs.nasa.gov/citations/19740022614 (Accessed: 11 August 2025).

Schneider, L. and La Hoz Theuer, S., 2019. Environmental integrity of international carbon market mechanisms under the Paris Agreement. Climate Policy, 19(3), pp.386-400. doi.org/10.1080/14693062.2018.1521332.

Tansey, K., Chambers, I., Anstee, A., Denniss, A. and Lamb, A., 2009. Object-oriented classification of very high resolution airborne imagery for the extraction of hedgerows and field margin cover in agricultural areas. Applied geography, 29(2), pp.145-157. doi.org/10.1016/j.apgeog.2008.08.004.

Tucker, C.J., 1979. Red and photographic infrared linear combinations for monitoring vegetation. Remote sensing of Environment, 8(2), pp.127-150. doi.org/10.1016/0034-4257(79)90013-0.

Valero, S., Chanussot, J., Benediktsson, J.A., Talbot, H. and Waske, B., 2010. Advanced directional mathematical morphology for the detection of the road network in very high resolution remote sensing images. Pattern Recognition Letters, 31(10), pp.1120-1127. doi.org/10.1016/j.patrec.2009.12.018.

Vannier, C. and Hubert-Moy, L., 2010, July. Wooded hedgerows characterization in rural landscape using very high spatial resolution satellite images. In 2010 IEEE International Geoscience and Remote Sensing Symposium (pp. 347-350). IEEE. doi.org/10.1109/IGARSS.2010.5651636.

Wang, L., Wang, J., Liu, Z., Zhu, J. and Qin, F., 2022. Evaluation of a deep-learning model for multispectral remote sensing of land use and crop classification. The Crop Journal, 10(5), pp.1435-1451. doi.org/10.1016/j.cj.2022.01.009.

Xiao, A., Xuan, W., Wang, J., Huang, J., Tao, D., Lu, S. and Yokoya, N., 2025. Foundation models for remote sensing and earth observation: A survey. IEEE Geoscience and Remote Sensing Magazine. doi.org/10.48550/arXiv.2410.16602.

Xie, Y., Sha, Z. and Yu, M., 2008. Remote sensing imagery in vegetation mapping: a review. Journal of plant ecology, 1(1), pp.9-23. doi.org/10.1093/jpe/rtm005.

Zhou, J., Cui, G., Hu, S., Zhang, Z., Yang, C., Liu, Z., Wang, L., Li, C. and Sun, M., 2020. Graph neural networks: A review of methods and applications. AI open, 1, pp.57-81. doi.org/10.1016/j.aiopen.2021.01.001.

Zhu, X.X., Tuia, D., Mou, L., Xia, G.S., Zhang, L., Xu, F. and Fraundorfer, F., 2017. Deep learning in remote sensing: A comprehensive review and list of resources. IEEE geoscience and remote sensing magazine, 5(4), pp.8-36. doi.org/10.1109/MGRS.2017.2762307.